Anal. Chem. **2003,** *75,* 5994−6001

Applications of Electron−Ion Dissociation Reactions for Analysis of Polycationic Chitooligosaccharides in Fourier Transform Mass Spectrometry

B. A. Budnik,[†,‡] K. F. Haselmann,[†] Yu. N. Elkin,[*,§] V. I. Gorbach,[§] and R. A. Zubarev[†,||]

Department of Chemistry, University of Southern Denmark, Campusvej 55, DK-5230, Odense M, Denmark, and Pacific Institute of Bioorganic Chemistry, Russian Academy of Sciences, Vladivostok, 690022, Russia

Singly protonated, doubly protonated, and sodiated pentaglucosamide $(GlcNAc)_5$, oligoglucosamines $(GlcN)_m$, and $(GlcN)_3GlcN(3OH14:0)$ were analyzed in an FTICR mass spectrometer by electron−ion dissociation reactions and compared to collision activation. The general fragmentation mode was found as the asymmetrical sequence fragments (B_n and minor C_n ion series) with full sequence coverage. Molecular mass information of each glucosamide or glucosamine residue can be readily obtained from the ion series. Fragmentation by electron capture dissociation revealed additional fragmentation of the *N*-acetyl moiety compared to sustained off-resonance irradiation collision-activated dissociation (SORI−CAD) and electron-induced dissociation (EID). Sodiated $GlcNAc_5$ molecular adduct ions were analyzed by EID and compared to CAD. Both techniques provided full sequence coverage. EID was more effective, but CAD resulted in the cross-ring ion products $^{0,2}A_n$ and $^{2,4}A_n$ for all relevant glucosamide residues.

Mass spectrometry (MS) is a powerful technique to analyze such challenging biomolecules as carbohydrate chains of glycans and glycoconjugates.[1−5] The complexity of oligosaccharides is much greater than peptides and DNA molecules due to the possibility of up to three substitutions on each monosaccharide unit, which can lead to a branched structure. The position of the substitution can be determined by high-energy collision-activated dissociation (HE CAD) via cross-ring cleavage in sodiated polysaccharides. However, HE CAD is unavailable on many modern instruments, where low-energy CAD (LE CAD) is used instead. Although LE CAD has been found to produce cross-ring cleavages of alcoholate anions[6] and sequence-specific fragments of sodiated underivatized oligosaccharides,[7] the occurrence of cross-ring cleavage is relatively rare in LE spectra. Furthermore, modern MS instrumentation often employs electrospray ionization (ESI) that produces abundant multiply protonated ions for molecules possessing groups with high proton affinities, such as amines.[8]

As model compounds, chitooligosaccharides (ChOSs) were selected as representatives of key carbohydrate structures involved in cell−cell signal transduction and isolated cell−environment signaling such as Nod factor,[9] lipid A,[10] and elsewhere O-chains of marine bacteria.[11] These molecules are predominantly hexosamine polymers or oligomers that are often O- and N-acylated e.g.. with fatty and amino acids. Since the Nod factor has a pentahexosamide backbone, it easily forms protonated molecular ions that in subsequent fragmentation by HE CAD created structurally significant product ions.[9] To the best of our knowledge, fragmentation of protonated ChOSs in HE CAD produces sequential cleavage of each glycosidic linkage with charge retention on the nonreducing side of the glycosidic linkage forming B-type ions (Domon and Costello nomenclature,[12] which can be viewed in the scheme of Figure 1a). This provides information on the number of residues and the size of their substitutions. Thus, we can recognize asymmetrical charge retention during sequencing of protonated ChOSs, whereas glycosidic cleavages of sodiated ChOSs are symmetric.[13]

* Corresponding author. E-mail: piboc@stl.ru.
† University of Southern Denmark.
‡ Current address: Department of Biochemistry, School of Medicine, Boston University, 650 Albany St. X-116, Boston, MA 02118.
§ Pacific Institute of Bioorganic Chemistry.
|| Current address: Laboratory for Biological and Medical Mass Spectrometry, Uppsala University, Box 534, SE-75121 Uppsala, Sweden.

(1) Burlingame, A. L.; Boyd, R. K.; Gaskell, S. G. *Anal. Chem.* **1994**, *66*, 634R-683R.
(2) Reinhold, V. N.; Reinhold, B. B.; Chan, S. In *Biological Mass Spectrometry: Present and Future*; Matsuo, N., Caprioli, R. M., Gross, M. L., Seyama, Y., Eds.; John Wiley & Sons: Chichester, U.K., 1994; pp 403−435.
(3) Reinhold, V. N.; Reinhold, B. B.; Costello, C. E. *Anal. Chem.* **1995**, *67*, 1772−1784.
(4) Reinhold, V. N.; Mühlecker, W.; Sheeley, D. M. In *Carbohydrate mass spectrometry in immunology and microbiology: sequencing with a quadruple ion trap;* Karjalainen, E. J., Heso, A. E., Jalonen, J. E., Karjalainen, U. P., Eds.; Elsevier Science Publishers: Amsterdam, 1998; Chapter 19, pp 462−473.
(5) Mirgorodskaya, E.; O'Connor, P. B.; Costello, C. E. *J. Am. Soc. Mass Spectrom.* **2002**, *13*, 318−324.
(6) Chai, W.; Piskarev, V.; Lowson, A. M. *Anal. Chem.* **2001**, *73*, 651−657.
(7) Bahr, U.; Pfenninger, A.; Karas, M. *Anal. Chem.* **1997**, *69*, 4530−4535.
(8) Zubarev, R. A.; Kelleher, N. L.; McLafferty, F. W. *J. Am. Chem. Soc.* **1998**, *120*, 3265−3266.
(9) van der Drift, K. M. G. M.; Olsthoorn, M. M. A.; Brüll, L. P.; Blok-Tip, L.; Thomas-Oates, J. E. *Mass Spectrom Rev.* **1998**, *17*, 75−95.
(10) Kaltashov, I. A.; Doroshenko, V.; Cotter, R. J. Takayama, K.; Qureshi, N. *Anal. Chem.* **1997**, *69*, 2317−2322.
(11) Haffinity, O. M.; Shashkov, A. S.; Senchenkova, S. N.; Tomshich, S. V.; Komandrova, N. A.; Romanenko, L. A.; Knirel, Y. A.; Savage, A. V. *Carbohydr. Res.* **1999**, *321*, 132−138.
(12) Domon, B.; Costello, C. E. *Glycoconjugate J.* **1988**, *5*, 397−409.
(13) Asam, M. R.; Glish, G. L. *J. Am. Soc. Mass Spectrom.* **1997**, *8*, 897−995.

10.1021/ac034477f CCC: $25.00
Published on Web 09/24/2003

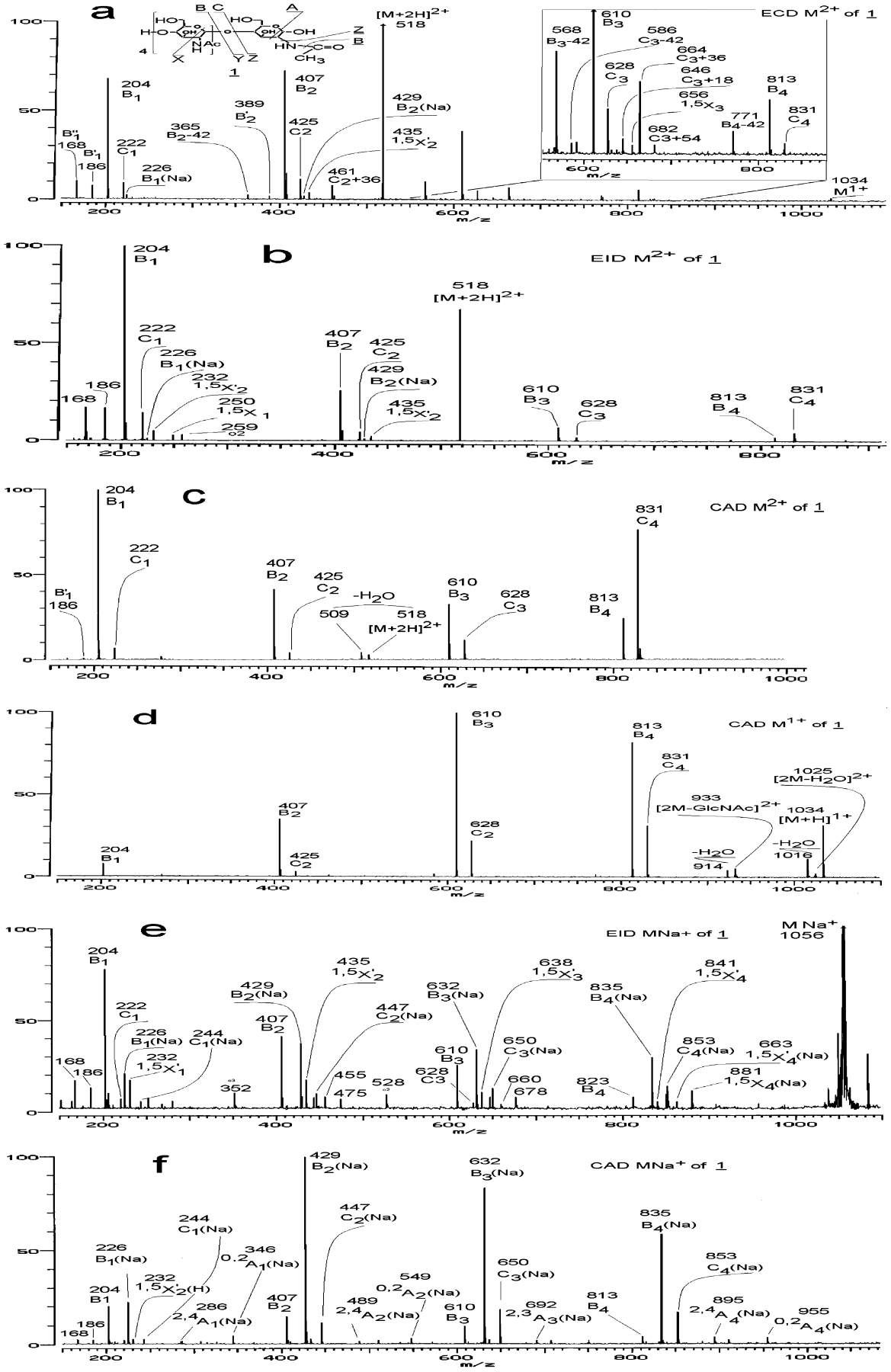

Figure 1. ESI FTICR MS/MS of $(GlcNAc)_5$ from **1**. ECD of MH_2^{2+} (a), EID of MH_2^{2+} (b), CAD of MH_2^{2+} (c), CAD of MH^+ (d), EID of MH^+ (e), and CAD of MNa^+ (f). Second and third harmonics are shown as o2 and o3, respectively, here and following figures.

The electron capture dissociation (ECD) technique has previously been applied to peptides,[8,14−16] proteins,[17−19] peptide nucleic acids,[20] and oxygenated species.[21,22] ECD is based on capture of low-energy electrons (<1 eV) by multiply protonated molecules $[M + nH]^{n+}$. The capture leads to formation of reduced radical ions $[M + nH]^{(n-1)\bullet+}$, which in the case of peptides rapidly dissociate via backbone $N-C_\alpha$ cleavage producing more complete and homogeneous sequence coverage than CAD. Recently, it has been found that even ~10-eV electrons can be captured; this hot electron capture dissociation produces far more abundant fragmentation than conventional ECD, with secondary fragmentation from the side chains that allows for distinguishing between the isomeric leucine and isoleucine residues.[23]

In this work, we investigated the question of whether ion−electron fragmentation techniques, such as ECD[8] of doubly protonated nitrogen-containing ChOSs, give new information compared to low-energy CAD in Fourier transform ion cyclotron resonance mass spectrometry (FTICR MS).

EXPERIMENTAL SECTION

Samples and Sample Preparation. The ChOSs studied were both modified natural and synthetic. The mixture of glucosamine oligomers $(GlcN)_m$, $4 \le m \le 13$, sample **2** was obtained from acidic degradation of chitosan followed by membrane separation and aqueous alcohol precipitation of the products. The pentamer glucosamide $(GlcNAc)_5$ sample **1** was generated from sample **2** by ion exchange chromatography followed by selective N-acetylation. Mono-*N*-3-hydroxyltetradecanoyl chitotetraose sample **3** was synthesized as described elsewhere.[24]

Mass Spectrometry. FTMS experiments were performed on an Ultima 4.7-T instrument (IonSpec, Irvine, CA) equipped with an ESI interface (Analytica of Branford, Branford, CT). The molecular ions were produced by nano-ESI using metallized pulled glass capillaries (Protana Engineering, Odense, Denmark). The precursor ions for fragmentation were isolated inside the Penning cell of the FTMS instrument by a preprogrammed waveform and irradiated by 1−14-eV electrons produced by an electron source based on an indirectly heated cathode.[14] For sustained off-resonance irradiation (SORI) CAD, a 500 ms rf burst with an amplitude of 6−8 V was applied at a frequency ~2 kHz higher than the m/z value of the molecular ions together with the pulse of a collision gas (4 ms of N_2 at 20 Torr). Monoisotope m/z values for ions are used in the text body, figures, and schemes.

Scheme 1

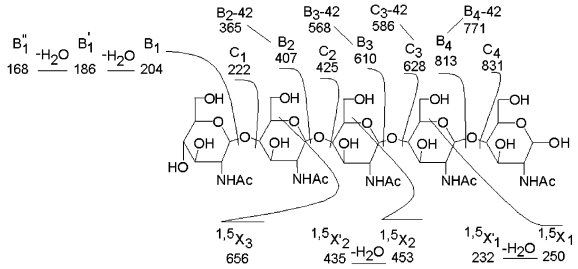

RESULTS AND DISCUSSION

Penta-*N*-acetylglucosamine $(GlcNAc)_5$ (1; Scheme 1): Electron Capture Dissociation. The capture of thermal electrons by isolated doubly charged penta-*N*-acetylglucosamine $(GlcNAc)_5$ (**1**) at m/z 518 caused reduction of its charge state and hydrogen desorption followed by extensive dissociation of glycosidic linkages (Figure 1a). None of the charge-reduced peak was visible, and only a very low abundance of the MH^+ species (m/z 1034) could be seen. McLafferty and co-workers reported the same observation that no reduced species were observed for electron capture dissociation of poly(ethylene glycol) molecules.[21,22] Here, the ECD spectrum demonstrated the most abundant ion series at m/z 204, 407, 610, and 813. This corresponds to glycosidic bond cleavage forming even-electron B_n-type ions. A less abundant ion series 18 Da higher can correspond to C_n-type ions, which resemble shortened saccharide chains. Both series could be either Z- or Y-type ions, respectively. However, the current assumption is the charge retention happens at the nonreducing end during fragmentation of protonated *N*-acetylaminoglycan molecules and will be discussed further below. Therefore, in the following discussion B_n- and C_n-type ions will be used. The abundance of B ions increased from the tetramer (m/z 813) to the monomer (m/z 204). The product ion at m/z 204 may be a B_1 ion, but some of the contribution could also be attributed to the presence of internal fragment ions. These fragment ions were most probably formed with excess internal energy, leading to the water loss fragments observed at m/z 186 and 168. The C_n ion series was formed in much lower abundance than the B ions. The C_4 ion (m/z 831), the highest mass member of the series, was observed only in low abundance. Thus, ECD caused cleavage of the doubly protonated $(GlcNAc)_5$ and resulted in many more nonreducing end fragments than in HE CAD of singly protonated analogues.[9] In the latter, no formation of the C_n/Y_n ions was observed at all.

Furthermore, the ECD spectrum of MH_2^{2+} from **1** revealed a B_n ($B_n - 42$) ion series at m/z 365, 568, and 771, which can be viewed as been generated from the B_n fragment ions (except B_1) by cleaving the amide bond with rearrangement of a hydrogen atom accompanied by loss of a ketene molecule (CH_2CO). The ratio $(B_n - 42)/B_n$ was 0.4 for $n = 4$ and decreased to 0.05 for $n = 2$. The most abundant fragment was the ($B_3 - 42$) (m/z 568). A peak at m/z 586 was also visible and could be considered to be the ($C_3 - 42$) originating from the C_3 ion Figure 1a (inset). Interestingly, a very weak (not really visible in Figure 1a unless

(14) Kruger, N. A.; Zubarev, R. A.; Horn, D. V.; McLafferty, F. W. *Int. J. Mass Spectrom.* **1999**, *185/186/187*, 787−793.
(15) Stensballe, A.; Jensen, O. N.; Olsen, J. V.; Haselmann, K. F.; Zubarev, R. A. *Rapid Commun. Mass Spectrom.* **2000**, *14*, 1793−1800.
(16) Axelsson, J.; Palmblad, M.; Håkansson, K.; Håkansson, P. *Rapid Commun. Mass Spectrom.* **1999**, *13*, 474−477.
(17) Kruger, N. A.; Zubarev, R. A.; Carpenter, B. K.; Kelleher, N. L.; Horn, D. M.; McLafferty, F. W. *Int. J. Mass Spectrom.* **1999**, *182/183*, 1−5.
(18) Zubarev, R. A.; Horn, D. M.; Fridriksson, E. K.; Kelleher, N. L.; Kruger, N. A.; Lewis, M. A.; Carpenter, B. K.; McLafferty, F. W. *Anal. Chem.* **2000**, *72*, 563−573.
(19) Horn, D. M.; Ge, Y.; McLafferty, F. W. *Anal. Chem.* **2000**, *72*, 4778−4784.
(20) Olsen, J. V.; Haselmann, K. F.; Nielsen, M. L.; Budnik, B. A.; Nielsen, P. E.; Zubarev, R. A. *Rapid Commun. Mass Spectrom.* **2001**, *15*, 969−974.
(21) Cerda, B. A.; Horn, D. M.; Breuker, K.; Carpenter, B. K.; McLafferty, F. W. *Eur. J. Mass Spectrom.* **1999**, *5*, 335−338.
(22) Cerda, B. A.; Breuker, K.; Horn, D. M.; McLafferty, F. W. *J. Am. Soc. Mass Spectrom.* **2001**, *12*, 565−570.
(23) Tsybin, Y. O.; Håkansson, P.; Budnik, B. A.; Haselmann, K. F.; Kjeldsen, F.; Gorshkov, M.; Zubarev R. A. *Rapid Commun. Mass Spectrom.* **2001**, *15*, 1849−1854.
(24) Gorbach, V. I.; Krasikova, I. N.; Luk'yanov, P. A.; Loenko, Yu. N.; Solov'eva, T. F.; Ovodov, Yu. S.; Deev, V. V.; Pimenov. A. A. *Carbohydr. Res.* **1994**, *260*, 73−82.

zooming in) ion series could be found at m/z 350, 553, and 756. These Z-type ions (taken from the peptide nomenclature) could be due to hydrogen attachment to the carbonyl group of the acetyl moiety followed by loss of the whole *N*-acetyl group including cleavage of the C1−O glycosidic bond. The B- and Z-type ions are the only fragment peaks differing from the other type of fragmentation done in this study, i.e., electron-induced dissociation (EID) and CAD.

Other observations in the ECD spectrum of MH_2^{2+} are the satellite peaks of the B and C ion series. The B_1-B_3 ions are accompanied by ions at which m/z values are 28 Da (m/z 232, 435, 638) higher. The $B_n + 28$ satellite ions can be assumed to be a $^{1,5}X_n$ ion series. These ions are also formed (see below) during EID and CAD of the singly, doubly protonated and sodiated $(GlcNAc)_5$ species. The ions are commonly observed independently from the kind of ion excitation (electron capture, irradiation, or collision). The ion series consists of ions at m/z 443, 461, 646, 664, and 682 and has additional ion series with masses 18, 36, and 54 Da higher than C_2 (m/z 425) and C_3 (m/z 628) ions. This low-abundant ion series appear to be water clusters of C_n ions; however, at the moment, it is difficult to rationalize their origin.

Electron-Induced Dissociation. An electron emitter with adjustable electron energy allows irradiating trapped ions with different electron energies (e.g., 10−13 eV), which exceeds the ionization energy of the analyte molecules (8−10 eV) but rather does not exeed the second energy ionization, which is unknown for such molecules. This hot electron irradiation provided diverse ionic types (MH_2^{2+}, MH^+, MNa^+) of the studied aminosaccharides. No ionization (see below) or electron capture was seen, only dissociation caused by electron impact vibrational excitation, and we call it here by the general term electron-induced dissociation. The EID spectrum of the dication (m/z 518) of **1** appeared in general like the ECD spectrum, except that the sequential fragmentation of glycosidic bonds is more extensive (Figure 1b). The abundant B_1 ion dominates the higher polymeric partners in the spectrum. The abundance of the B ions decreased monotonically from B_1 to B_4. Another peculiarity is the relatively high abundance of C_n fragments, all of roughly equal abundance. There are no other types of ions in the spectrum except the $^{1,5}X_2$ ion (m/z 250) and a water loss product (m/z 232). EID of MH^+ (not shown) gave a product ion spectrum that looked more like the ECD spectrum than the EID of the protonated dication. Thus, both electron capture and electron impact of ChOSs provided full sequence coverage.

Collision-Activated Dissociation. CAD of both doubly and singly protonated species of $(GlcNAc)_5$ provided more simple product ion spectra (Figure 1c and d) than EID or ECD had done. Beside two common B_n/C_n series, there are minor losses of water molecules only. The relative yield of the abundant B_n and C_n ions differs from the ECD and EID (Figure 1a and b). CAD of the dications resulted in abundant B_1 (m/z 204) ions similar to those observed for ECD and EID. However, the abundance of the C_n ions demonstrated an opposite effect: the C_4 (m/z 831) was the second most abundant fragment peak in the spectrum after the B_1 ion. Here, it is also relevant to note that the ratio C_4/B_4 in the EID (Figure 1b) and in the CAD spectra (Figure 1c) of the protonated dications has nearly the same value. Observation of the same types of fragments, except for the abundances, in both CAD and EID spectra suggests that the same type of excitation takes place, e.g., vibrational excitation.

The CAD spectrum of the MH^+, m/z 1034, is simpler than the EID spectrum of the same molecular ion (Figure 1d). Particularly, there are substantially reduced satellite ions that accompanist the fragment ions. However, in the spectrum, a few doubly charged ions can be observed. These ions are believed to originate from fragmentation of the doubly charged dimer of $(GlcNAc)_{10}$, also present in the electrospray source spectrum and having the same m/z value. The distribution of B ions markedly differs form the one that could be observed in the EID spectrum of the same species. The B_4 (m/z 610) and B_3 (m/z 813) ions have the highest abundance, whereas in ECD and EID, the most abundant fragments were the nonreducing terminus B_1 (m/z 204) ion. Formation of the C_3 and C_4 ions during CAD of both singly and doubly protonated molecular species is apparently a favorable process. This process did not occur at all under high-energy collision conditions in sector instruments.[9] But C_n ions can be observed in HE CAD spectra.[5] All three dissociation techniques applied to protonated ChOSs resulted in full sequence coverage.

EID and CAD of Sodiated Molecules. Metal ion (Na^+) complexations can be considered as weak modifications of the electron properties of the ligand monosaccharide residues. Such modification of oligosaccharides can generate structural formation by meaningful cross-ring fragmentation during CAD.[12] Fragmentation of sodiated $(GlcNAc)_5$ was done by both SORI CAD and EID (∼11 V) techniques. In addition to the expected $B_n(Na)/C_n(Na)$ ion series, both techniques provided B and C ions that are not sodiated and are also observed in HE CAD spectra of sodiated precursors despite careful isolation of parent ions (Figure 1e and f). The protonated types, especially B_1 (m/z 204) and B_2 (m/z 407), are the most abundant peaks in the EID spectrum of MNa^+. Thus, EID and CAD of sodiated parent ions provided full sequence coverage. However, electron irradiation was more effective for sequencing protonated ions, and numerous satellite peaks accompany cleavages of the glycosidic bonds.

In the CAD spectrum (Figure 1e) of MNa^+ (m/z 1056), the sequence ions have relative abundances that are similar to the singly protonated species (Figure 1d). This indicates that the patterns of formation of B/C ions do not relate to the charge carried by the ChOS molecule. Sodium complexation of the ChOS chain promoted the $^{0,2}A_n$ and $^{2,4}A_n$ cross-ring fragmentation in all rings during CAD, when 10-V excitation amplitude was applied (Figure 1f). However, in the case when collision energy was reduced (5-V amplitude), then cross-ring fragmentation provided only lowest mass fragments $^{0,2}A_1$ and $^{2,4}A_1$ at m/z 346 and 286, respectively.

Heptaglucosamine $(GlcN)_7$ (2; Scheme 2). Hexosamine chains of N-deacetylated ChOSs $(GlcN)_m$, where $m = 3-13$, from **2** are weak cationic biopolymers and provided abundant multiply charged gaseous ions in ESI mass spectrometry. The maximum charge density was two protons per three GlcN residues. The two most abundant doubly charged molecular peaks were m/z 493 and 574 in the ESI profile, corresponding to m equal to 6 and 7, respectively. The doubly charged heptamer $(GlcN)_7$ was isolated, and it was used as representative for aminoglycans in this study. However, as only dications were observed for these species, the

Scheme 2

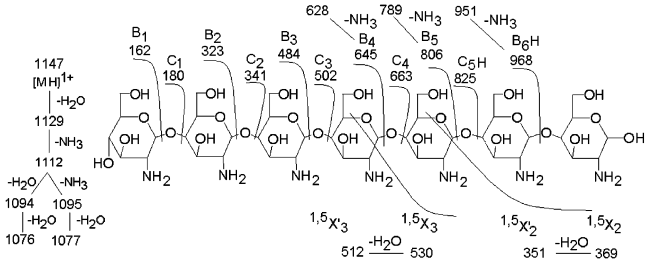

$(GlcN)_m$ ($m = 4$ and 5) from **2** were used in fragmentation studies of singly charged polyhexosamines.

Electron Capture Dissociation. ECD of MH_2^{2+} (m/z 574), $GlcN_7$, showed the same common B ion pattern as the main product ions (Figure 2a). In this spectrum, the reduced molecular peak could not be observed ($[M + 2H]^{+\bullet}$ at m/z 1148), as in the previous case. Only the MH^+ (m/z 1147), corresponding to proton desorption, was observed. However, some differences in the ECD spectra between **1** and **2** were observed. The relative abundances of B_n ions from $GlcN_7$ are lower and increase with increasing number of residue units (m), whereas in the ECD profile of $(GlcNAc)_5$, a nearly opposite pattern was observed. Abundant losses of both water (−18 Da) and ammonia (−17 Da), accompanying B_n ion formation, are prominent in the spectrum of $(GlcN)_7$, particularly in the high-m/z region. The loss of ammonia is typically seen in ECD of amine-containing species, including peptides. Here, the MH^+ ion showed up to four sequential losses of both water and ammonia. These losses decrease when the number of residues of B_n ions decrease. However, for $(GlcNAc)_5$, only B_n ($n = 1$ and 2) ions that were formed with enough excess energy were able to lose water and no ammonia molecules (Figure 1a). A peculiarity is the observation of the odd-electron species at m/z 968 and 825 corresponding to B_6H and C_5H, which are 1 Da higher than conventional sequence ions. Rearrangement of a "hot" hydrogen atom from a hypervalent species upon electron capture that eventually would lead to cleavage of the glycosidic bond is a tentative explanation of this observation. However, it is only observed for $(GlcN)_7$ and not for $(GlcNAc)_5$.

Electron-Induced Dissociation. Irradiation of the same dications (m/z 574) as above with 11-eV electrons provided only singly charged product ions in the EID spectrum (Figure 2b) similar to the amide analogues (**1**). The EID spectrum demonstrates the same tendency of intensive cleavage of glycosidic linkages and accumulation of B_1 ions. The abundances of the nonreduced end B_n ion series are gradually decreasing as the number of residues goes up. Such a pattern for a ladder of B_n ions is a consequence of vibrational excitation of the parent ion. The other primary fragmentation channel is formation of the cross-ring X_n ($n = 2$ and 3) ion series at m/z 351, 369 and 512, 530, respectively. In Figure 2b, the odd-electron species B_6H^+ (m/z 968) and C_5H^+ (m/z 826) are also evident, indicating that electron capture took place. A high degree of sequential ammonia and then water losses is seen in the spectrum, particularly from B ions. Minor loss of water was also observed from the isolated parent ion, m/z 565.

The singly charged species of $(GlcN)_5$ from **2** was also isolated and irradiated with electrons (11 eV) (spectrum not shown). Here, the same dissociation pattern as the dications of $(GlcN)_7$ were observed.

Collision-Activated Dissociation. CAD of MH_2^{2+} (m/z 574) provided predominantly singly charged fragment ions and demonstrated a clear pattern of protonated aminoglycan fragmentation (Figure 2c). However, the surviving fraction of the MH_2^{2+} ions successfully dissociated, and two doubly charged sequence ions $B_5H_2^{2+}$ and $C_6H_2^{2+}$ at m/z 403 and 493, respectively, were obtained. Only B- and C-type ions were detected, except for minor losses of NH_3 of B fragment ions as well. Compared to the EID spectrum, the losses of ammonia (m/z 306, 467, 628, and 789) were less abundant. This observation can be explained by the formation of fragments with less excess energy. In SORI CAD, the internal energy is readily adjusted. From the parent ion, abundant (up to three) water losses are observed and the first water loss is the base peak in the spectrum. The relative distribution of B_n and C_n ions occurs similar to that in the EID spectrum with only slight variations. The B_3 ion (m/z 484) was the second most abundant peak in the B series. The relative abundances of the C_n ions are almost constant for residue numbers $n = 3$, 4, and 5. Similar CAD results were obtained for singly charged $(GlcN)_5$, m/z 824 and $(GlcN)_4$, m/z 663 species.

Lipotetraglucosamine ($GlcN_4$-$COCH_2CHOHC_{11}H_{25}$) (3; Scheme 3). Since the ChOSs studied so far are symmetric, an unambiguous identification of the B-/Z-type ions and the Y-/C-type ions cannot be done, even despite the assumption, based on the HE CAD study of protonated pentaChOS amide analogues.[9] An asymmetric chain is needed to remove the symmetry degeneration for the glycosidic cleavage of the ChOS chains. The $(GlcN)_3$-$GlcNCOCH_2$ $CH(OH)C_{11}H_{25}$) of **3** was used. This ChOS has an amine group at the reducing terminus modified by acylation with 3-tetradecanoic acid (increment 226 Da). The ESI profile of **3** contains both $[MH]^{1+}$ (m/z 889) and at higher abundance MH_2^{2+} (m/z 445) molecular ion species.

Electron Capture Dissociation. ECD of the dication (m/z 445) provided full sequence coverage (Figure 3a). The singly charged molecular ion (m/z 889) from which water loss occurred, but the reduced parent ion $[M + 2H]^{\bullet+}$ which was not observed in the previous cases was also absent. The spectrum showed a variable asymmetric charge (proton) distribution over four possible sequence product ions from glycosidic cleavage. B ions at m/z 484, 323, and 162 provided the main product ions with decreasing abundances, respectively. The C_2 (m/z 341) fragment is the most abundant of the C_n-type ions. The complementary sequence ions of Z and Y ions are also formed upon electron capture. The Y_2 (m/z 567) and Z_1 (m/z 388) ions are the most abundant sequence ions of the reduced end series. However, their total relative abundances are rather low. The formation of the B_n- and C_n-type ions are more favorable processes. The B_3 (m/z 484) fragment is the main product ion. This ion also loses ammonia, and when many scans were coadded and averaged, a small peak corresponding to water loss from B_2 and B_3 ions could be observed.

The preferential formation of B and C fragment ions at lower m/z in the ECD spectrum of this asymmetric molecule makes the assumption in the previous cases valid. Thus, electron capture by multiply charged ChOS amine chains predominantly causes cleavage of the saccharide chains via inner glycosidic bond

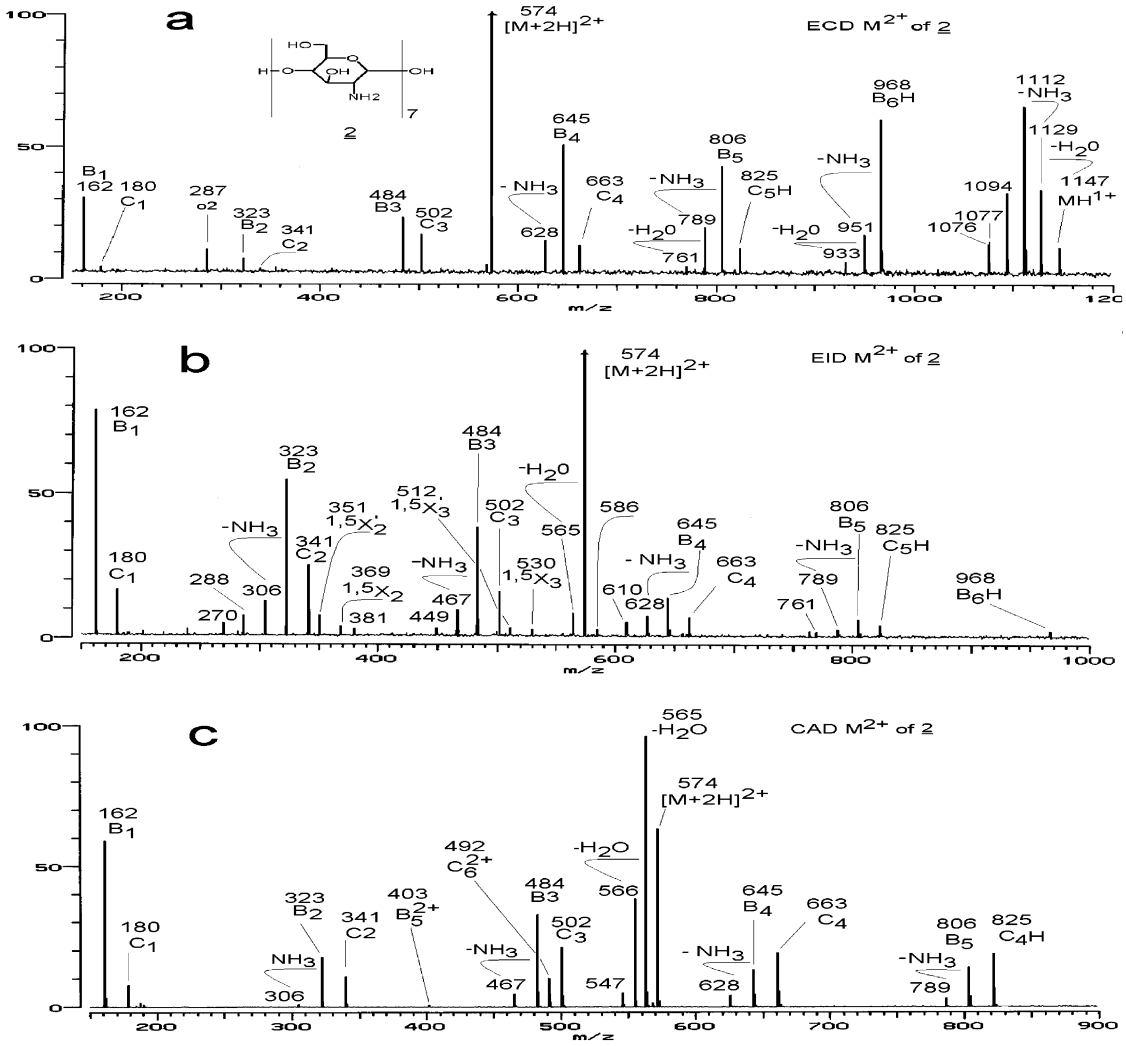

Figure 2. ESI FTICR MS/MS of $(GlcN)_7$ from **2**. ECD of MH_2^{2+} (a), EID of MH_2^{2+} (b), and CAD of MH_2^{2+} (c).

Scheme 3

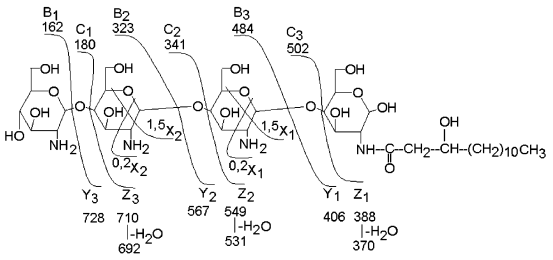

cleavage with favorable formation of B-type ions. That are stabilized by participation of the 2-amino group.

Electron-Induced Dissociation. Energetic electron irradiation (acceleration voltage 8−13 V) of MH_2^{2+} and MH^+ demonstrated in both spectra full sequence coverage (Figure 3b and c). B ions are still the most favorable products during electron irradiation. The most abundant fragment peak in Figure 3b is the B_1 ion (m/z 162) and from that the abundance decreases near linearly. In dissociation of the singly charged cation (Figure 3c), this observation is reversed. Again formation of the reduced end fragment ions Z_n and Y_n were seen in the EID spectra of, especially, the singly protonated species (Figure 3c). Abundances of these ions are low compared to B ions and are comparable to the abundances of the C ions. Only one Y_n ($n = 1$) ion was seen in Figure 3b and was of very low abundance. The relative abundances between the B/C ions and the Y/Z ions are fairly equal.

In Figure 3b and d, B ions 1 Da lighter (B − 1) than conventional fragments were observed. These peaks at m/z 161, 322, and 483 were also observed in the EID spectrum of MH^+ of **2**. The abundances were low and the measured mass difference from the B_n ion was 1.008 ± 0.002 Da, corresponding to loss of a hydrogen atom. It is assumed that the B − 1 ions are real oxonium ions O_n^+ caused by electron ionization of the O-atom of the ether. These oxonium ions were not found in the ECD and the CAD spectra of MH_2^{2+} of **1** and **2** because their formation required electron excitation higher than the energy ionization of the ion. The energetic (13 eV) electrons are able to induce the cross-ring cleavage in MH^+ ion of lipotetraglucosamine **3**. The small peaks m/z 595, 607 and 756, 768 of $^{1,5}X_n$ ($n = 2, 3$) and $^{0,2}X_n$ ($n = 2, 3$) ion series, respectively, were recorded (Figure 3d).

Collision-Activated Dissociation. CAD of protonated species MH_2^{2+} and MH^+ (Figure 3e and f) showed a charge-dependent dissociation. The dication (m/z 445) was cleaved predominantly on the first glycosidic linkage and the complimentary B_1 and Y_3 ions were produced. A similar pattern can be seen in Figure 1c

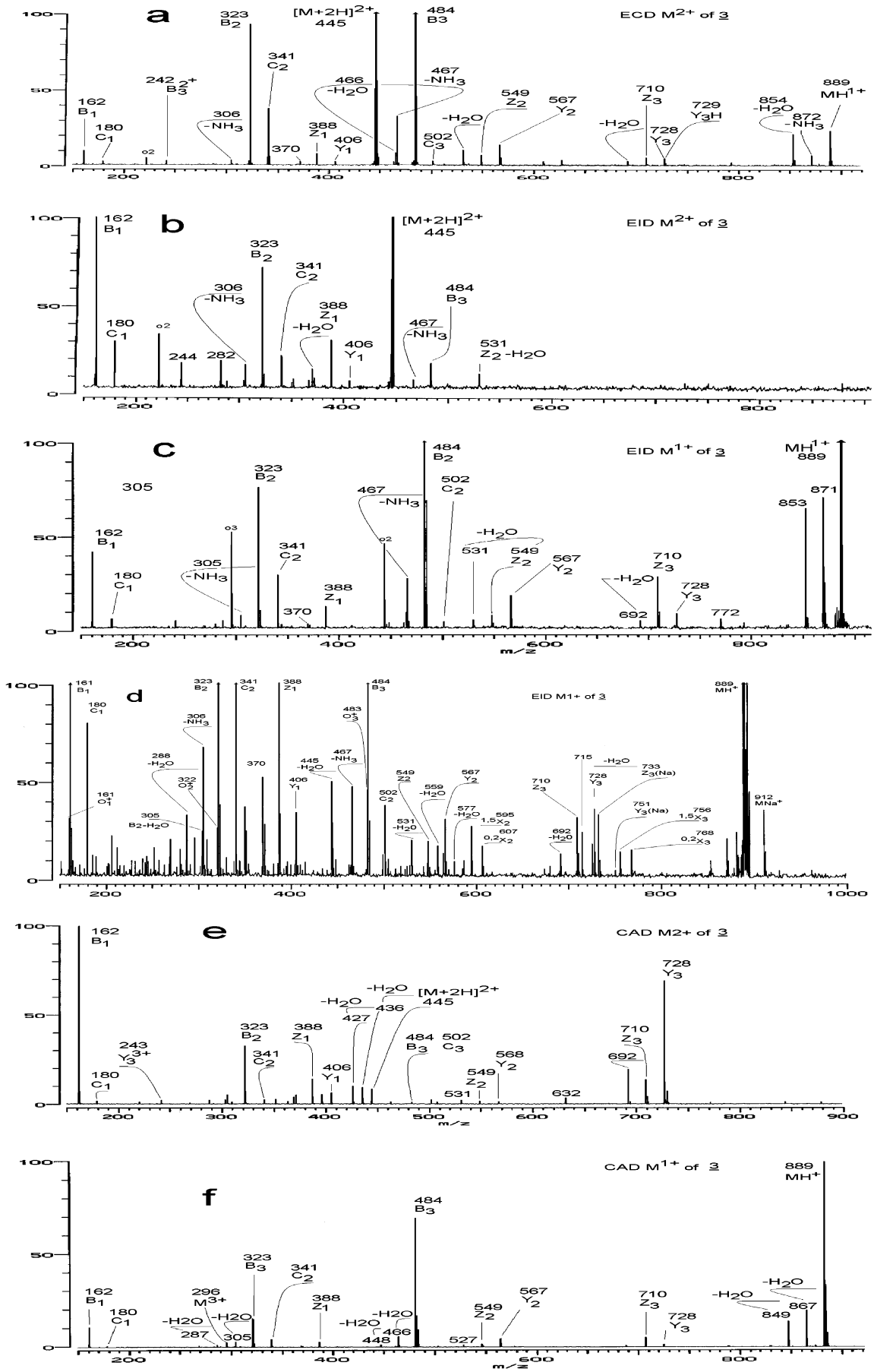

Figure 3. ESI FTICR MS/MS of $(GlcN)_3GlcNHCOCH_2CHOHC_{11}H_{25}$ from **3**. ECD of MH_2^{2+} (a), EID of MH_2^{2+} (b), EID of MH^+ (c), EID of MH^+, 1s acquisition by 13-eV electrons (d), CAD of MH_2^{2+} (e), and CAD of MH^+ (f).

and to a lesserextent in Figure 2c (CAD of MH_2^{2+} from **1** and **2**, respectively) under condition of existence of symmetry degeneration for B/Z and C/Y ion formation. This means ions C_4, m/z 831 (Figure 1c), and C_5H, m/z 825 (Figure 2c), both shared their ion currents with ions Y_4 and Y_5H, respectively. The excess of abundance for lower ions of the Y_n-type over that for ions of the C_n-type (Figure 3c) does not means that there is an analogue that partitions between congeners that formed from **1** and **2** (Figures 2c and 3c), which are marked as C_n ions. Such disproportion could be caused by an asymmetrical acylation pattern of tetraglucosamine **3**. Actually, sodiated *reduced* aminated GlcNHAc chains produced predominantly Y_n-type ions in the gas plume of the MALDI source under an uncertain nature of activation.[25] CAD of the initial sodiated chitobiose[26] and C4-substituted by trimannose antennas[27,28] demonstrated a drastic abundance difference for B_n and Y_1 ions. To our knowledge, the CAD of $GlcNH_2$ chains was not studied elsewhere. The singly charged cation (m/z 889) dissociates at the third glycosidic linkage and produces only B_3 ion, m/z 484, in high abundance (Figure 3f). Formation under CAD conditions is accompanied by loss of water molecules, whereas the EID spectra provide loss of NH_3 from the B_3 ion as well.

CONCLUSION

The range ECD, EID, and CAD tandem mass spectrometric analysis of glycoconjugates composed of aminosaccharide residues revealed full sequence coverage in the positive ion mode of both protonated and sodiated species. In general, preferential formation of the nonreducing end B fragment ions was observed in all spectra. However, all types of glycosidic bond cleavage (B/C and Y/Z) could be observed. Variations occurred according to which fragmentation technique was used and which species were selected for fragmentation. In ECD of the doubly protonated ChOSs, hydrogen desorption resulted in the formation of mostly B and minor C ions. Additionally, fragmentation of the *N*-acetyl moiety resulted in loss of ketene and a minor abundance acetamide except for both terminus acetamide residues. Nearly the same abundance of B and a minor level of C ions were observed in EID, which, in addition, produced minor odd-electron species 1 Da lighter. Enough energetic electrons caused a weak tendency toward cross-ring cleavage of the inner $GlcNH_2$ residues with charge retention on the reducing end moiety. In CAD, the fragmentation patterns were more charge dependent, and for doubly protonated species, heterolytic cleavage with charge separation producing B_n and Y_{m-n} fragments was a feasible process, whereas, for the singly protonated species, C ion fragments were also abundant. Furthermore, sodiated species gave CAD cross-ring fragments ($^{0,2}A_n$ and $^{2,4}A_n$) for all relevant glucosamine residues except the distal residue.

(25) Bahrke, S.; Einarsson, J. M.; Gislason, J.; Haebel, S.; Kathalinic, J. P. Peter, M. G. Proceeding 5th Int. Conf. Eur. Chitin Soc., Trondheim, 2002; pp 3−10.
(26) Cancilla, M. T.; Wong, A. W.; Voss, L. R.; Lebrilla, C. B. *Anal. Chem.* **1999**, *71*, 3206−3218.
(27) Cancilla, M. T.; Penn, S. G.; Carroll, J. A.; Lebrilla, C. B. *J. Am. Chem. Soc.* **1996**, *118*, 6736−6745.
(28) Harvey, D. J. *J. Mass Spectrom.* **2000**, *35*, 1178−1190.

ACKNOWLEDGMENT

The authors acknowledge Prof. Catherine E. Costello for valuable discussions and correct nomenclature for the oligosaccharides fragmentation pattern. The FTMS instrument was funded by the Instrument Center Program (Grant 9700471) and related programs (Grants SNF 9801448 and STVF 0001242).

Received for review May 6, 2003. Accepted August 14, 2003.

AC034477F